České vysoké učení technické v Praze
Fakulta jaderná a fyzikálně inženýrská

Czech Technical University in Prague
Faculty of Nuclear Sciences and Physical Engineering

RNDr. Petr Sváček, PhD.

Numerické řešení aeroelastických problémů metodou konečných prvků

Numerical solution of aeroelastic problems by finite element method

Summary: This paper is devoted to the topic of mathematical modelling and numerical simulation of the interaction of two dimensional incompressible viscous flow and a vibrating structure. A solid airfoil with two degrees of freedom is considered. The numerical simulation consists of the finite element solution of the Navier-Stokes equations coupled with the system of ordinary differential equations describing the airfoil motion. The time dependent computational domain and a moving grid are taken into account with the aid of the Arbitrary Lagrangian-Eulerian (ALE) formulation of the Navier-Stokes equations. High Reynolds numbers up to 10^6 require the application of a suitable stabilization of the finite element discretization. Here, the modified Galerkin Least-Squares stabilization is applied and modified within the context of ALE formulation of Navier-Stokes system of equations. The fluid model is coupled with the nonlinear structure model for the solid airfoil. The method is applied on several technical problems.

Souhrn: Tato práce se zabývá modelováním a numerickou simulací interakce nestlačitelné vazké tekutiny a struktury. Je uvažován model tuhého leteckého nosníku se dvěmi stupni volnosti. Numerická simulace se sestává z aproximace Navierových-Stokesových rovnic pomocí metody konečných prvků spojeného se systémem diferenciálních rovnic popisující pohyb nosníku. Problém časově proměnné oblasti je řešen pomocí Arbitrary Lagrangian-Eulerian (ALE) formulace Navierových-Stokesových rovnic. Vysoká Reynoldsova čísla (až 10^6) vyžadují aplikaci vhodné metody stabilizace. Zde je použita modifikovaná Galerkinova Least-Squares metoda stabilizace a použita na ALE formulaci Navierových-Stokesových rovnic. Model tekutiny je spojen s nelineárním modelem popisujícím pohyb leteckého nosníku. Výsledná metoda je použita na vybrané technické problémy.

Klíčová slova: Arbitrary Lagrangian-Eulerian metoda, nestlačitelné proudění, metoda konečných prvků

Keywords: Arbitrary Lagrangian-Eulerian method, incompresssible flow, finite element method

Contents

1 Introduction

The interaction of fluid flow and an elastic structure plays an important role in many technical disciplines - airplane industry (e.g., wings deformations), blade machines (turbines, compressors, pumps), civil engineering (stability of bridges), etc. The interaction between moving fluids and vibrating structures is usually studied [see, e.g., [4], [11]]. In technical applications typically only special problems of aeroelasticity or hydroelasticity are solved mainly limited to linearized models with the consideration of small deformations. Flutter at large deformations can be studied by analytical methods [9] only in some special cases. The real situation is usually much more complicated. It is necessary to consider viscous flow, changes of the flow domain in time, turbulence effects, nonlinear behaviour of the elastic structure and to solve simultaneously the evolution systems for the fluid flow and for the oscillating structure.

This paper focuses on the numerical simulation of aeroelastic problem of two-dimensional viscous incompressible air flow and an airfoil with two or three degrees of freedom. The airfoil is considered as a solid flexibly supported body, allowing vertical and torsional vibrations. Transient motion of the airfoil before or after the loss of stability is addressed.

The mathematical model of the fluid flow is represented by the system consisting of the 2-D Navier-Stokes equations and the continuity equation, equipped with initial conditions and mixed boundary conditions. For approximation the finite element method is applied, but for the incompressible flow problem several important obstacles need to be overcome. First, it is necessary to take into account that the finite element velocity/pressure pair has to be suitably chosen in order to satisfy the Babuška-Breezi condition, which guarantees the stability of the scheme – see, e.g., [13] or [14]. Further, the dominating convection requires the introduction of some stabilization of the finite element scheme. Here the residual based stabilization is employed, cf. [6]. Moreover, it is necessary to design carefully the computational mesh, using adaptive grid refinement in order to allow an accurate resolution of time oscillating thin boundary layers, wakes and vortices. In our case we use the anisotropic mesh adaptation technique of [3] for the construction and adaptive refinement of the mesh.

Due to the motion of the airfoil, the computational domain is time-dependent. This requires to use techniques working on moving meshes. A suitable choice is to apply the Arbitrary Lagrangian-Eulerian (ALE) method, which is based on the reformulation of the Navier-Stokes equations (12, 10) using an ALE mapping of the reference configuration onto the current configuration for the time under consideration. The ALE formulation of the Navier-Stokes equations is coupled with the structural model, describing the airfoil vibrations.

2 Mathematical model

2.1 ALE method

In order to simulate flow in a moving domain, we employ the Arbitrary Eulerian-Lagrangian (ALE) method, based on an ALE mapping

$$\mathcal{A}_t : \Omega_0 \to \Omega_t, \quad \xi \mapsto x(\xi, t) = \mathcal{A}_t(\xi), \tag{2.1}$$

of the reference configuration $\Omega_{\mathrm{ref}} = \Omega_0$ onto the current configuration Ω_t.

Any function $f = f(x,t)$ defined for and $t \in \mathfrak{I}$ and $x \in \Omega_t$ can be transformed on the original configuration Ω_0. The transformed function will be denoted by $\widehat{f} = \widehat{f}(\xi, t)$ defined for any $t \in \mathfrak{I}$ and $\xi \in \Omega_0$ by equation

$$\widehat{f}(\xi, t) = f(\mathcal{A}_t(\xi), t). \tag{2.2}$$

Further, by the time derivative of the ALE mapping $\mathcal{A}_t$ we get the *domain velocity* $\mathbf{w}_D = \mathbf{w}_D(x,t)$ defined for any $t \in \mathfrak{J}$ and $x \in \Omega_t$, i.e.

$$\mathbf{w}_D(x,t) = \frac{\partial \mathcal{A}_t(\xi)}{\partial t}, \qquad \text{where } x = \mathcal{A}_t(\xi). \tag{2.3}$$

Further, the time derivative with the respect to the reference configuration Ω_0 is called the *ALE derivative* $D^{\mathcal{A}}/Dt$, i.e.

$$\frac{D^{\mathcal{A}} f}{Dt}(x,t) \quad = \quad \frac{\partial \widehat{f}}{\partial t}(\xi, t), \qquad x = \mathcal{A}_t(\xi),$$

where functions $\widehat{f}$ and f satisfy equation (2.2). The ALE derivative and the time derivative are related by

$$\frac{D^{\mathcal{A}} f}{Dt}(x,t) = \frac{\partial f}{\partial t}(x,t) + \mathbf{w}_D(x,t) \cdot \nabla f(x,t), \tag{2.4}$$

where $\mathbf{w}_D$ is the domain velocity defined by (2.3).

2.2 Fluid model

In the domain Ω_t we consider the Navier-Stokes system written in the ALE form, cf. [12]:

$$\frac{D^{\mathcal{A}}}{Dt}\mathbf{v} + [(\mathbf{v} - \mathbf{w}_D) \cdot \nabla] \mathbf{v} + \nabla p - \nu \triangle \mathbf{v} = 0, \tag{2.5}$$

$$\nabla \cdot \mathbf{v} = 0, \tag{2.6}$$

where $\mathbf{v}$ is the fluid velocity, p is the kinematice pressure, and ν is the kinematic viscosity. To equation (2.5) we add the initial condition

$$\mathbf{v}(x, 0) = \mathbf{v}_0, \quad x \in \Omega_0, \tag{2.7}$$

and boundary conditions

$$\begin{array}{lll} \text{(a)} & \mathbf{v}|_{\Gamma_D} = \mathbf{v}_D, & \text{(b)} \quad \mathbf{v}|_{\Gamma_{Wt}} = \mathbf{w}_D|_{\Gamma_{Wt}}, \\ \text{(c)} & -(p - p_{\mathrm{ref}})\mathbf{n} + \nu \dfrac{\partial \mathbf{v}}{\partial \mathbf{n}} = 0 \quad \text{on } \Gamma_O. & \end{array} \tag{2.8}$$

Here $\mathbf{n}$ is the unit outer normal to the boundary $\partial\Omega_t$ of the domain Ω_t, Γ_D represents the inlet (and, possibly, fixed impermeable walls), Γ_O is the outlet and Γ_{Wt} is the boundary of the airfoil at time t. Condition (2.8b) represents the assumption that the fluid adheres to the airfoil. We denote by p_{ref} a prescribed reference outlet pressure. The choice of a suitable boundary condition on the outlet is a delicate question. In order to allow a good resolution of a wake propagation through the outlet, we use here the "soft" boundary condition (2.8c).

2.3 Structure model

A solid flexibly supported airfoil is shown in Figur 2.1. The airfoil can be vertically displaced and rotated. The nonlinear equations of motion of the airfoil reads (see [5])

$$\begin{aligned} m\,\ddot{h} + S_\alpha\,\ddot{\alpha}\,\cos\alpha - S_\alpha\,\dot{\alpha}^2\,\sin\alpha + k_{hh}\,h &= -L(t), \\ S_\alpha\,\ddot{h}\,\cos\alpha + I_\alpha\ddot{\alpha} + k_{\alpha\alpha}\,\alpha &= M(t). \end{aligned} \tag{2.9}$$

In order to evaluate the aerodynamical forces one needs to start with the definition of the airfoil boundary Γ_{Wt} (the airfoil boundary moves in time).

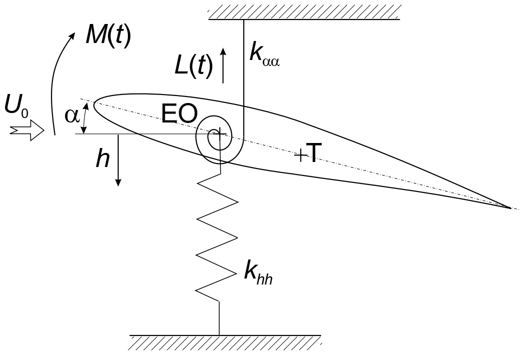

Figure 2.1: The elastic support of the airfoil on translational and rotational springs.

Then, the aerodynamical lift force L acting in the vertical direction, and the torsional moment M are defined by

$$L = -\, l \int_{\Gamma_{Wt}} \sum_{j=1}^{2} \tau_{2j} n_j \,\mathrm{dS}, \qquad M = l \int_{\Gamma_{Wt}} \sum_{i,j=1}^{2} \tau_{ij} n_j r_i^{\mathrm{ort}} \,\mathrm{dS}, \quad (2.10)$$

where

$$\tau_{ij} = \rho \left[-p\delta_{ij} + \nu \left(\frac{\partial v_i}{\partial x_j} + \frac{\partial v_j}{\partial x_i} \right) \right], \quad (2.11)$$
$$r_1^{\mathrm{ort}} = -(x_2 - x_{\mathrm{EO2}}),\ r_2^{\mathrm{ort}} = x_1 - x_{\mathrm{EO1}},$$

and $x_{\mathrm{EO}} = (x_{\mathrm{EO1}}, x_{\mathrm{EO2}})$ is the position of the elastic axis (lying in the interior of the airfoil).

3 Numerical approximation

3.1 Time discretization

We consider a partition $0 = t_0 < t_1 < \cdots < T,\ t_k = k\tau$, with a time step $\tau > 0$, of the time interval $[0, T]$ and approximate the solution $\mathbf{v}(\cdot, t_n)$ and $p(\cdot, t_n)$ (defined in Ω_{t_n}) at time t_n by $\mathbf{v}^n$ and p^n, respectively. For the time discretization we employ a second-order two-step scheme using the computed approximate solution $\mathbf{v}^{n-1}$ in $\Omega_{t_{n-1}}$ and $\mathbf{v}^n$ in Ω_{t_n} for the calculation of $\mathbf{v}^{n+1}$ in the domain $\Omega_{t_{n+1}} = \Omega_{n+1}$.

Then, on each time level t_{n+1}, the second-order two-step ALE time discretization yields the problem of finding unknown functions $\mathbf{v}^{n+1} : \Omega_{t_{n+1}} \to R^2$ and $p^{n+1} : \Omega_{t_{n+1}} \to R$ satisfying the equations

$$\begin{aligned} &\frac{3\mathbf{v}^{n+1} - 4\widehat{\mathbf{v}}^{n} + \widehat{\mathbf{v}}^{n-1}}{2\tau} + \left(\left(\mathbf{v}^{n+1} - \mathbf{w}_D^{n+1}\right) \cdot \nabla\right) \mathbf{v}^{n+1} - \nu \Delta \mathbf{v}^{n+1} + \nabla p^{n+1} = 0, \\ &\operatorname{div} \mathbf{v}^{n+1} = 0, \end{aligned} \tag{3.1}$$

in $\Omega_{t_{n+1}}$, and the boundary conditions (2.8).

3.2 Weak formulation

We define for a fixed time $t = t_{n+1}$ the finite element velocity spaces $\mathcal{W}, \mathcal{X}$ by

$$\mathcal{W} = \mathbf{H}^1(\Omega_{t_{n+1}}), \qquad \mathcal{X} = \left\{ \mathbf{z} \in \mathcal{W} \, : \mathbf{z} = 0 \text{ on } \Gamma_D \cup \Gamma_{W t_{n+1}}, \right\},$$

and the pressure space

$$\mathcal{Q} = L^2(\Omega_{t_{n+1}}).$$

We approximate the ALE velocity $\mathbf{w}_D(t_{n+1})$ by $\mathbf{w}_D^{n+1}$ and set $\widehat{\mathbf{v}}^i = \mathbf{v}^i \circ \mathcal{A}_{t_i} \circ \mathcal{A}_{t_{n+1}}^{-1}$. The vector-valued functions $\widehat{\mathbf{v}}^i$ are defined in the domain $\Omega_{t_{n+1}}$.

The weak formulation of the time discretized problem then reads:

Problem 3.1. *Find $U = (\mathbf{v}, p)$ such that satisfies*

$$\mathsf{a}(U; U, V) = f(V), \qquad \textit{for all } \; V = (\mathbf{z}, q) \in \mathcal{X} \times \mathcal{Q}, \tag{3.2}$$

and conditions (2.8a,b). The forms are defined for $U = (\mathbf{v}, p)$, $V = (\mathbf{z}, q)$, $U^* = (\mathbf{v}^*, p)$ by

$$\begin{aligned} \mathsf{a}(U^*; U, V) &= \left(\frac{3\mathbf{v}}{2\tau}, \mathbf{z}\right)_{\Omega_{n+1}} + \int\limits_{\Omega_{n+1}} ((\mathbf{v}^* - \mathbf{w}_D^{n+1}) \cdot \nabla)\mathbf{v} \cdot \mathbf{z} \, \mathrm{dx} + \\ &\quad + \nu \left(\nabla \mathbf{v}, \nabla \mathbf{z}\right)_{\Omega_{n+1}} - (p, \operatorname{div} \mathbf{z})_{\Omega_{n+1}} + (\operatorname{div} \mathbf{v}, q)_{\Omega_{n+1}} \qquad (3.3) \\ f(V) &= \int_{\Omega_{n+1}} \frac{4\widehat{\mathbf{v}}^{n} - \widehat{\mathbf{v}}^{n-1}}{2\tau} \cdot \mathbf{z} \, \mathrm{dx} - \int_{\Gamma_{out}} p_{\mathrm{ref}} \mathbf{z} \cdot \mathbf{n} \; dS. \end{aligned}$$

3.3 Space discretization

In order to apply the Galerkin FEM, we approximate the spaces $\mathcal{W}$, $\mathcal{X}$, $\mathcal{Q}$ from the weak formulation by finite dimensional subspaces $\mathcal{W}_\triangle$, $\mathcal{X}_\triangle$, $\mathcal{Q}_\triangle$, $\triangle \in (0, \triangle_0)$, $\triangle_0 > 0$, $\mathcal{X}_\triangle = \{\mathbf{v}_\triangle \in \mathcal{W}_\triangle; \mathbf{v}_\triangle|_{\Gamma_D \cap \Gamma_{Wt}} = 0\}$. The couple $(\mathcal{X}_\triangle, \mathcal{Q}_\triangle)$ of the finite element spaces should satisfy the Babuška–Brezzi (BB) condition [see, e.g., [7], [8] or [17]]. In practical computations we assume that the domain Ω_{n+1} is a polygonal approximation of the region occupied by the fluid at time t_{n+1} and the spaces $W_\triangle$, $\mathcal{X}_\triangle$, $\mathcal{Q}_\triangle$ are defined over a triangulation $\mathcal{T}_\triangle$ of the domain Ω_{n+1}, formed by a finite number of closed triangles $K \in \mathcal{T}_\triangle$. We use the standard assumptions on the system of triangulation. Here $\triangle$ denotes the size of the mesh $\mathcal{T}_\triangle$. The spaces $W_\triangle$, $\mathcal{X}_\triangle$ and $\mathcal{Q}_\triangle$ are formed by piecewise polynomial functions. In our computations, the well-known Taylor-Hood P_2/P_1 conforming elements are used for the velocity/pressure approximation: The approximate solutions of the time-discretized problem (3.1) will be sought in the spaces $\mathcal{X}_\triangle$ and $\mathcal{W}_\triangle$ defined by

$$\begin{array}{c} \mathcal{H}_\triangle = \{v \in C(\overline{\Omega_{n+1}}); v|_K \in P_{k+1}(K) \text{ for each } K \in \mathcal{T}_\triangle\}, \\ \mathcal{W}_\triangle = [\mathcal{H}_\triangle]^d, \qquad\qquad \mathcal{X}_\triangle = \mathcal{W}_\triangle \cap \mathcal{X}, \\ \mathcal{Q}_\triangle = \{v \in C(\overline{\Omega_{n+1}}); v|_K \in P_k(K) \text{ for each } K \in \mathcal{T}_\triangle\}. \end{array} \tag{3.4}$$

Further, the dominating convection requires to introduce some stabilization of the finite element scheme, as, e.g. upwinding or streamline-diffusion method. Here, the modified Galerkin-Least Squares stabilization method is applied, cf. ([6]). We start with the definition of the *local element rezidual*s: the local element rezidual terms $\mathcal{R}_K^{\mathsf{a}}$ and $\mathcal{R}_K^f$ are defined in the interior of the element $K \in \mathcal{T}_\triangle$ by

$$\begin{aligned} \mathcal{R}_K^{\mathsf{a}}(\tilde{\mathbf{w}}; \mathbf{v}, p) &= \frac{3\mathbf{v}}{2\Delta t} - \nu \triangle \mathbf{v} + \left(\overline{\mathbf{w}}^{n+1} \cdot \nabla\right) \mathbf{v} + \nabla p, \\ \mathcal{R}_K^f(\hat{\mathbf{v}}_n, \hat{\mathbf{v}}_{n-1}) &= \frac{1}{2\Delta t}(4\hat{\mathbf{v}}_n - \hat{\mathbf{v}}_{n-1}). \end{aligned}$$

The stabilization terms are defined as

$$\begin{aligned} \mathcal{L}(U_\triangle^*; U_\triangle, V_\triangle) &= \sum_{K \in T_\triangle} \delta_K \Big(\mathcal{R}_K^{\mathsf{a}}(\tilde{\mathbf{w}}; \mathbf{v}, p), \left(\overline{\mathbf{w}}^{n+1} \cdot \nabla\right) \mathbf{z} + \nabla q\Big)_K, \\ \mathcal{F}(V_\triangle) &= \sum_{K \in T_\triangle} \delta_K \Big(\mathcal{R}_K^f(\hat{\mathbf{v}}_n, \hat{\mathbf{v}}_{n-1}), \left(\overline{\mathbf{w}}^{n+1} \cdot \nabla\right) \mathbf{z} + \nabla q\Big)_K, \end{aligned} \tag{3.5}$$

where the function $\overline{\mathbf{w}}^{n+1}$ stands for the transport velocity, i.e. $\overline{\mathbf{w}}^{n+1} = \mathbf{v}^* - \mathbf{w}_D^{n+1}$. Moreover, the additional grad-div stabilization

$$\mathcal{P}_\triangle(U, V) = \sum_{K \in \mathcal{T}_\triangle} \tau_K (\operatorname{div} \mathbf{v}, \operatorname{div} \mathbf{z})_K, \tag{3.6}$$

is introduced with suitably chosen parameters $\tau_K \geq 0$. The choice of the parameters δ_K and τ_K is carried out according to [6] or [15]:

$$\delta_K = \delta^* h_K^2, \qquad \tau_K = \tau^*, \tag{3.7}$$

where $\tau^* > 0$ and $\delta^* > 0$ are fixed constants.

Problem 3.2 (SUPG stabilized discrete problem)**.** *The SUPG stabilized discrete problem reads: Find $U_\triangle = (\mathbf{v}_\triangle, p_\triangle) \in \mathcal{W}_\triangle \times \mathcal{Q}_\triangle$ such that $\mathbf{z}_\triangle$ satisfies approximately conditions (2.8), a), c) and*

$$\begin{aligned} &\mathsf{a}(U_\triangle; U_\triangle, V_\triangle) + \mathcal{L}_{SUPG}(U_\triangle; U_\triangle, V_\triangle) + \mathcal{P}_\triangle(U_\triangle, V_\triangle) = f(V_\triangle) + \mathcal{F}_{SUPG}(V_\triangle) \\ &\qquad \textit{for all } \ V_\triangle = (\mathbf{z}_\triangle, q_\triangle) \in \mathcal{X}_\triangle \times \mathcal{Q}_\triangle. \end{aligned} \tag{3.8}$$

4 Numerical Results

4.1 Dynamic effects

First, the comparison of the computed pressure coefficients for the NACA 0012 profile with theoretical and experimental results from [16] and [1] is shown. The chord of the airfoil is $c = 0.1122$ m, the prescribed oscillations are defined by $\alpha = \alpha_0 \sin(2\pi t/f)$, the frequency $f = 30$ Hz, the far-field velocity $U_\infty = 136$ m/s and the elastic axis is located at 25% of the chord measured from the leading edge. In Figures 4.1 – 4.1, we present the distribution of the mean value of the pressure coefficient c_p, its real part c_p' and imaginary part c_p'' in dependence on the length of the chord measured from the leading edge for $\alpha_0 = 1°$.

4.2 Stall flutter simulations

Further, numerical simulation of flow past the NACA0012 profile with a prescribed vibration around the elastic axis was carried out. The profile rotation was considered according to the formula $\alpha = 10(1 + \sin(2\pi t/f))$

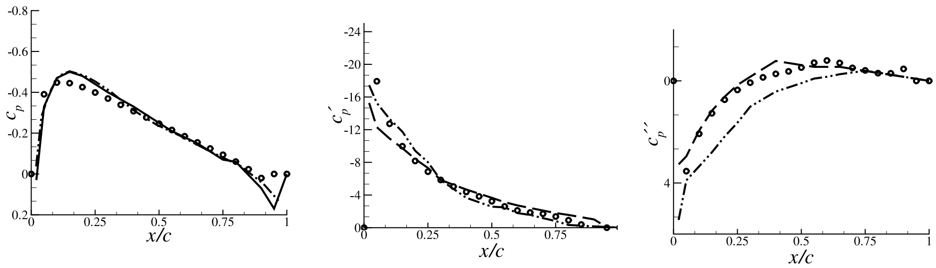

Figure 4.1: The mean value of the pressure coefficient c_p, real part c_p' and imaginary part c_p''.

with frequency $f = U_\infty/(2\pi c)$, where c is the airfoil chord and the Reynolds number $\mathrm{Re} = 5 \times 10^3$. This type of process was examined experimentally and the results are contained in [11, Section 7.3.2]. In Figures 4.2 – 4.2 we present flow patterns, which we computed for several angles of attack. The agreement with experimental results from [11] is very good.

4.3 Aeroelastic computations

Predominant mode shape	**Eigenfrequency for $U_\infty = 0$**	**Critical flow velocity U_∞**	**Instability type**	**Flutter frequency**
Translation	$f_1 = 5.537\,\mathrm{Hz}$	$37.7\,\mathrm{m\,s^{-1}}$	Divergence	0 Hz
Rotation	$f_2 = 13.98\,\mathrm{Hz}$	$42.4\,\mathrm{m\,s^{-1}}$	Flutter	8.93 Hz

Table 1: The results obtained by NASTRAN code for the aeroelastic case.

Further, the aeroelastic simulations were performed for the airfoil NACA $63_2 - 415$. The following quantities are considered: $m = 0.086622$ kg, $S_\alpha = -0.000779673$ kg m, $I_\alpha = 0.000487291$ kg m^2, $k_{hh} = 105.109$ N/m, $k_{\alpha\alpha} = 3.695582$ N m/rad, $l = 0.05$ m, $c = 0.3$ m, $\rho = 1.225$ kg/m^3, $\nu = 1.5 \cdot 10^{-5}$ m/s^2. The position of the elastic axis EO and the centre of gravity T of the airfoil measured along the chord from the leading edge are $\mathrm{x}_T = 0.37c = 0.111$ m and $\mathrm{x}_{EO} = 0.4c = 0.12$ m, respectively.

The simulation of fluid-structure interaction as a function of time is shown in Figures 4.3- 4.6. The left and right panels show the angle of rotation α and the vertical displacement h, respectively.

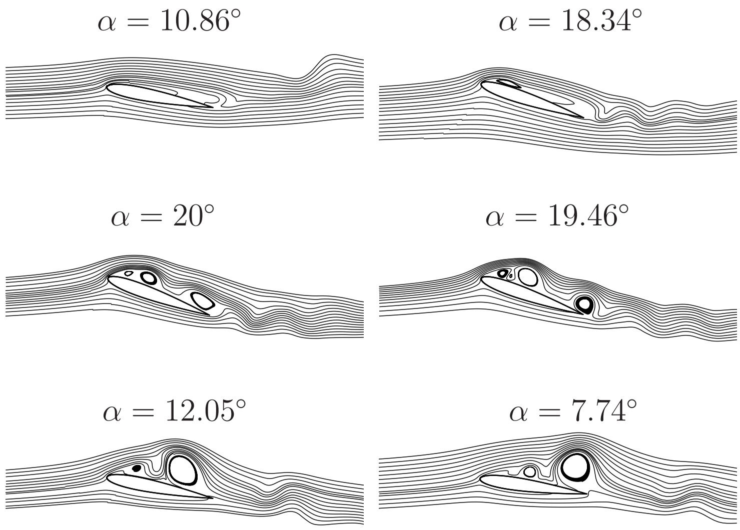

Figure 4.2: Streamlines of the flow around a moving airfoil for an angle of attack.

For lower velocities the vibrations die out in time and the system is stable. For flow velocities higher than 32 m/s, one can observe the influence of vortices separating from the airfoil. For $U_\infty \geq 40$ m/s we get an unstable behaviour with large airfoil displacements.

In [2], the NASTRAN flutter analysis carried out with the aid of the strip model for the fluid flow is presented. The NASTRAN calculations are summarized in Table 1. According to this table the critical velocities are $U_\infty = 37.7$ m/s for divergence and $U_\infty = 42.4$ m/s for flutter, which correspond to our results.

5 Conclusion

The robust finite element method (FEM) for the numerical simulation of interaction of incompressible flow and a vibrating airfoil is presented. It is based on the combination of several techniques: the Arbitrary Lagrangian-Eulerian (ALE) formulation of the laminar Navier-Stokes equations, suitable time discretization, the finite element method using velocity/pressure finite element pairs satisfying the Babuška–Brezzi condition, stabilization of the

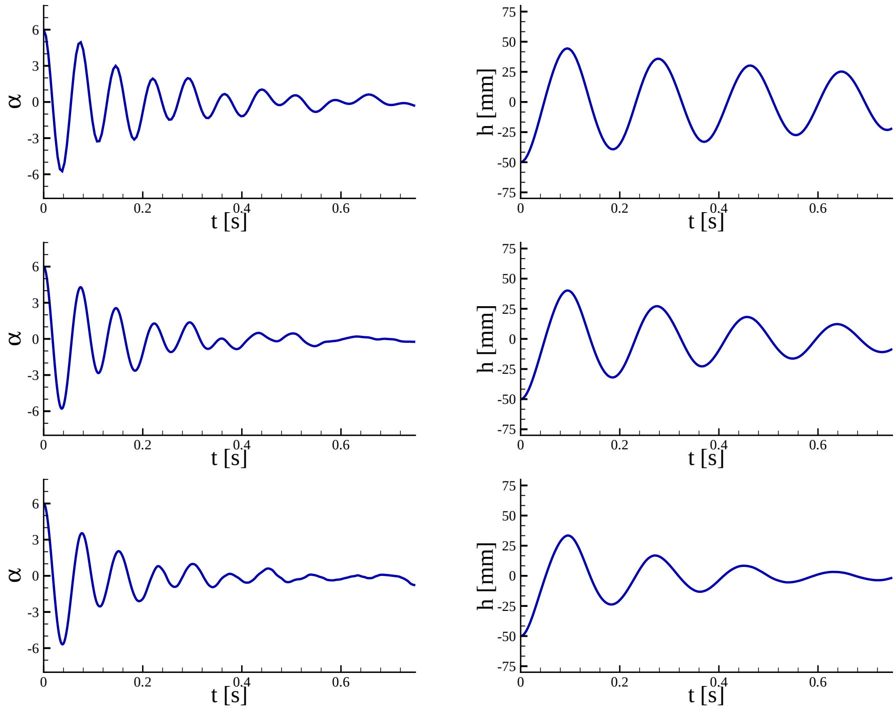

Figure 4.3: Divergence type instability. System response for $U_\infty = 2$ m/s, $U_\infty = 8$ m/s, $U_\infty = 14$ m/s and $U_\infty = 20$ m/s m/s (respectively from the top to the bottom).

finite element scheme, linearization of the discrete nonlinear problem, a fast linear solver, the numerical scheme for the solution of ordinary differential equations describing the vibrations of the airfoil and sufficiently accurate method for the evaluation of fluid dynamical forces acting on the airfoil.

References

[1] J. Benetka, J. Kladrubský, and R. Valenta. Measurement of NACA 0012 profile in a slotted measurement section. Technical Report R-2909/98, Aeronautical Research and Test Institute, Prague, Letňany (in Czech), 1998.

[2] J. Čečrdle and J. Maleček. Verification FEM model of an aircraft construction with two and three degrees of freedom. Technical Report R-

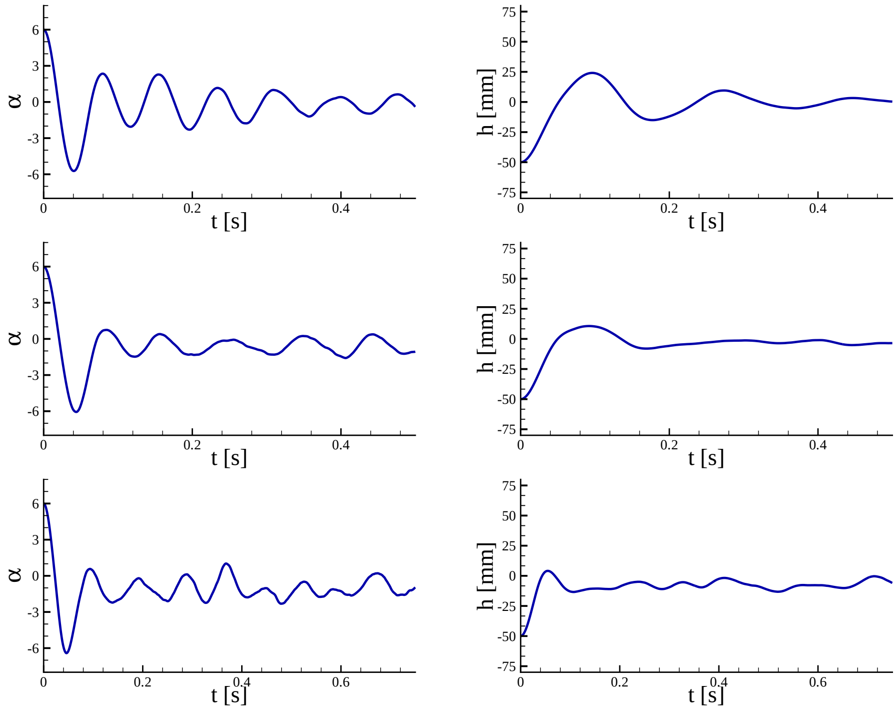

Figure 4.4: Divergence type instability. System response for $U_\infty = 20$ m/s, $U_\infty = 26$ m/s and $U_\infty = 32$ m/s (respectively from the top to the bottom).

3418/02, Aeronautical Research and Test Institute, Prague, Letňany (in Czech), 2002.

[3] V. Dolejší. Anisotropic mesh adaptation technique for viscous flow simulation. *East-West Journal of Numerical Mathematics*, 9:1–24, 2001.

[4] E. H. Dowell. *A Modern Course in Aeroelasticity*. Kluwer Academic Publishers, Dodrecht, 1995.

[5] M. Feistauer, J. Horáček, and P. Sváček. Numerical simulation of flow induced airfoil vibrations with large amplitudes. *Journal of Fluids and Structure*, 23(3):391–411, 2007. ISSN 0889-9746.

[6] T. Gelhard, G. Lube, M. A. Olshanskii, and J.-H. Starcke. Stabilized finite element schemes with LBB-stable elements for incompressible flows. *Journal of Computational and Applied Mathematics*, 177:243–267, 2005.

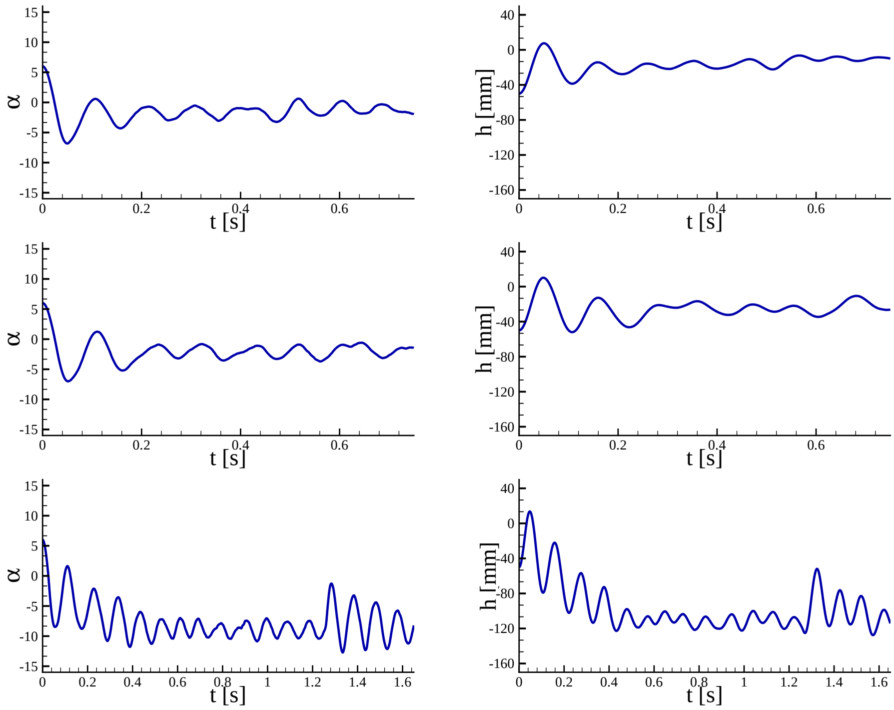

Figure 4.5: Divergence type instability. System response for $U_\infty = 36$ m/s, $U_\infty = 38$ m/s and $U_\infty = 40$ m/s.

[7] V. Girault and P.-A. Raviart. *Finite Element Methods for the Navier-Stokes Equations*. Springer-Verlag, Berlin, 1986.

[8] P. M. Gresho and R. L. Sani. *Incompressible Flow and the Finite Element Method*. Wiley, Chichester, 2000.

[9] P. Holmes and J. E. Marsden. Bifuraction to divergence and flutter in flow-induced oscillations: an infinite dimensional analysis. In *Control of Distributed parameter Systems, Proceedings of 2nd IFAC Symposium*, pages 133–145, Coventry, Great Britain, 1977.

[10] P. Le Tallec and J. Mouro. Fluid structure interaction with large structural displacements. *Computer Methods in Applied Mechanics and Engineering*, 190:3039–3067, 2001.

[11] E. Naudasher and D. Rockwell. *Flow-Induced Vibrations*. A.A. Balkema, Rotterdam, 1994.

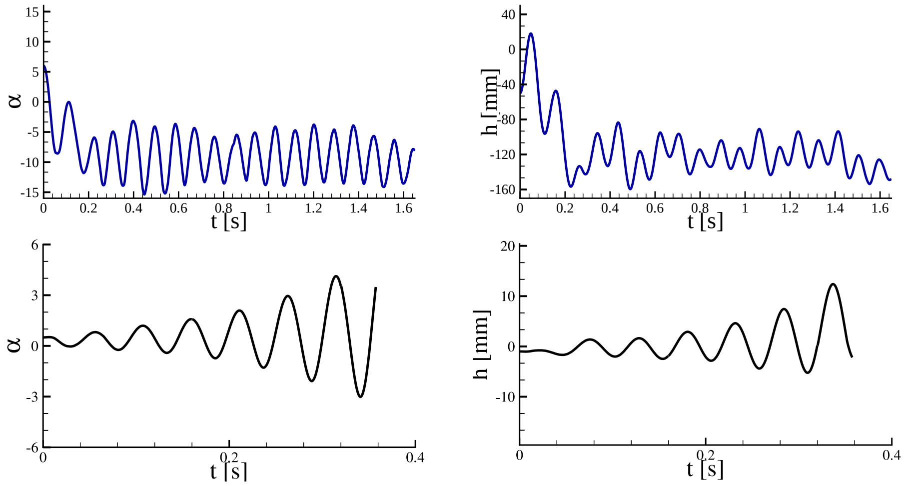

Figure 4.6: Divergence type instability. System response for $U_\infty = 42$ m/s and $U_\infty = 45$ m/s.

[12] T. Nomura and T. J. R. Hughes. An arbitrary Lagrangian-Eulerian finite element method for interaction of fluid and a rigid body. *Computer Methods in Applied Mechanics and Engineering*, 95:115–138, 1992.

[13] P.-A. Raviart and V. Girault. *Finite Element Methods for the Navier-Stokes Equations*. Springer, Berlin, 1986.

[14] R. L. Sani and P. M. Gresho. *Incompressible Flow and the Finite Element Method*. Wiley, Chichester, 2000.

[15] P. Sváček and M. Feistauer. Application of a Stabilized FEM to Problems of Aeroelasticity. In *Numerical Mathematics and Advanced Application*, pages 796–805, Berlin, 2004. Springer.

[16] H. Triebstein. Steady and unsteady transonic pressure distributions on naca 0012. *Journal of Aircraft*, 23:213–219, 1986.

[17] R. Verfürth. Error estimates for mixed finite element approximation of the Stokes equations. *R.A.I.R.O. Analyse numérique/Numerical analysis*, 18:175–182, 1984.

RNDr. Petr Sváček, PhD.

Petr Sváček se narodil 19.1.1973. Vystudoval v letech 1991-1996 matematicko-fyzikální fakultu UK Praha (obor numerická matematika). V letech 1993-1997 pracoval na částečný úvazek na geofyzikálním ústavu AV ČR, kde se zabýval aplikací numerických metod v problémech geodynama.

Počínaje rokem 1996 pokračoval v postgraduálním studiu na katedře numerické matematiky na MFF UK Praha v oboru vědeckotechnické výpočty. V roce 2002 úspěšně obhájil disertační práci „Finite element method on problems with nonlinear boundary conditions".

Od roku 2001 je zaměstnán na ústavu technické matematiky na fakultě strojní ČVUT v Praze. Zde se zaměřuje zejména na aplikace metody konečných prvků, numerické řešení aeroelastických problémů a problémů proudění tekutiny. V letech 2005-2006 absolvoval jednoletou stáž na pozici visiting assistant profesor na University of Texas at El Paso, Department of Mathematical Sciences, El Paso, Texas, USA.

O svých výsledcích referoval na více než 20-ti mezinárodních konferencích, např. ENUMATH 2003 v Praze, Flow Induced Vibrations 2004, v Paříži, ACOMEN 2005 v Gentu, ENUMATH 2005 v Santiago de Compostela, BAIL 2006 v Gottingenu, ECCOMAS CFD 2006 v Egmond am See, 4th MIT Conference on Fluids and Solids v Bostonu, ENUMATH 2007 v Grazu. Je autorem a spoluautorem více než 50 publikací publikovaných jak ve sbornících prestižních konferencích tak i v recenzovaných a impaktovaných časopisech.